ARTICLE TYPE

Size and shape effects on thermodynamic properties of nanoscale volumes of water[†]

Bjørn A. Strøm,[*a] Jean-Marc Simon ,[b] Sondre K. Schnell,[c] Signe Kjelstrup, [d] Jianying He,[a] and Dick Bedeaux,[d]

Small systems are known to deviate from the classical thermodynamic description, among other things due to their large surface area to volume ratio compared to corresponding big systems. As a consequence, extensive thermodynamic properties are no longer proportional to the volume, but are instead higher order functions of size and shape. We investigate such functions for second moments of probability distributions of fluctuating properties in the grand-canonical ensemble, focusing specifically on the volume and surface terms as proposed by Hadwiger [Hadwiger, Springer, 1957]. We resolve the shape dependence of the surface term and show, using Hill's nanothermodynamics [Hill, J. Chem. Phys., 1962, **36**, 3182], that the surface satisfies the thermodynamics of a flat surface as described by Gibbs [Gibbs, Ox Bow Press, 1993, **Vol. 1**]. The Small System Method (SSM), first derived by Schnell et al. [Schnell et al., J. Phys. Chem. B, 2011, **115**, 10911], is extended and used to analyze simulation data on small systems of water. We simulate water as an example to illustrate the method, using the TIP4P/2005 and other models, and compute the isothermal compressibility and thermodynamic factor. We are able to retrieve the experimental value of the bulk phase compressibility within 2 %, and show that the compressibility of nanosized volumes increases by up to a factor of two as the number of molecules in the volume decreases. The value for a tetrahedron, cube, sphere, polygon, etc. can be predicted from the same scaling law, as long as second order effects (nook and corner effects) are negligible. Lastly, we propose a general formula for finite reservoir correction to fluctuations in subvolumes.

1 Introduction

Classical thermodynamics is the well-established framework for classifying and interpreting chemical and physical properties, but it applies only to systems that are sufficiently large. In thermodynamics, a system is considered small when thermodynamic variables such as internal energy and enthalpy are no longer propor-

[a] Department of Structural Engineering, Faculty of Engineering Science and Technology, Norwegian University of Science and Technology, Trondheim, Norway. E-mail: bjorn.a.strom@ntnu.no
[b] Laboratoire Interdisciplinaire Carnot de Bourgogne, UMR 6303, CNRS-Université de Bourgogne, 9, av. Savary, 21000 Dijon, France.
[c] Department of Materials Science and Engineering, Faculty of Natural Sciences, Norwegian University of Science and Technology, Trondheim, Norway.
[d] Department of Chemistry, Faculty of Natural Science and Technology, Norwegian University of Science and Technology, Trondheim, Norway.

tional to the volume V[1]. For such systems, extensive variables are higher order functions of size and shape, and the classical thermodynamic equations cannot be applied without modifications. For small systems there is, for instance, an energy contribution proportional to the surface area[1] $\Omega \sim V^{2/3}$. Such size effects can be significant. A systematic method that deals with these effects, is the topic of this paper.

Terrell L. Hill generalized in 1962 the Gibbs equation of classical thermodynamics, to apply also for small systems. In doing so, he initiated the development of what is now referred to as nanothermodynamics or the thermodynamics of small systems[1–4].

Following Hill's formalism, Schnell et al. derived in 2011 a method to obtain macroscopic thermodynamic properties from local fluctuations in density and energy, using molecular dynamics simulations[5]. By embedding small non-periodic systems in a

larger periodic reservoir, they showed that the properties of the small systems at fixed chemical potential and temperature, indeed differed from those of periodic bulk systems. By systematically varying the size of the embedded systems, several of the properties derived from the local fluctuations were found, in good approximation, to be linear in the inverse cube root of the volume. The linear relation could be extrapolated to obtain thermodynamic limit values. In this manner, the partial enthalpy[6] and the thermodynamic factor[5] were efficiently obtained from local fluctuations. Similarly, Kirkwood-Buff integrals were obtained for mixtures[7,8]. The non-periodic boundary condition of the small system, produces an entropy of the surface, different from the bulk entropy, dependent on system size and shape. An investigation on the details of the surface effect and higher order terms related to the shape was initiated, and laid the groundwork for further results[9].

In this work we further develop the method and the systematic description of thermodynamic properties of small systems, using the specific treatment of volume and surface terms for extensive quantities as proposed by Hadwiger[10]. We investigate the shape dependence of the surface term and show, using Hill's nanothermodynamics, that the surface satisfies the thermodynamics of a flat surface as described by Gibbs[4]. We show that the first and second moments of the particle - and energy - density distributions are the fundamental quantities from which we can obtain volume and surface terms separately. The second moments are related to the fluctuations that naturally arise when the particles are free to move in and out of the small system. The relations between these and the thermodynamic properties of the small system can best be obtained using Hill's nanothermodynamics. We further show how the partial enthalpy, thermodynamic factor, and the isothermal compressibility can be obtained by combination of the fundamental quantities. Improvements in the derivation, compared to earlier work, shall be pointed out.

With two exceptions[8,11], previous work has mainly focused on short-range interaction models. As a natural progression of these studies, we chose to calculate the fundamental quantities for models simulated with long-range electrostatic interactions, specifically the common water models SPC/E[12], TIP3PEw[13], TIP4PEw[14] and TIP4P/2005[15].

Using the TIP4P/2005 water model, we calculate the volume and surface contributions to the isothermal compressibility. The model is able to accurately reproduce the experimental values of the compressibility in the thermodynamic limit. The equivalence of Hill's and Gibbs' thermodynamics leads us to hypothesize that the information we gain from local fluctuations in small volumes of water is related to formation of droplets or bubbles within bulk phases, however, this idea requires further research.

This paper is organized as follows: In Sec. 2, we review the thermodynamics of small systems as developed by Hill. In Sec. 3,

we develop the description of thermodynamic variables in terms of volume and surface contributions. Sec. 4 derives the equations relating fluctuations in the grand-canonical ensemble to the volume and surface term description of thermodynamic variables. Sec. 5 describes the details of the simulation setup, the methodology and the parameters of the water models we have used. In Sec. 6 we present the simulation results for a selection of common water models, demonstrating the shape dependence of particle and energy fluctuations. We follow this by a subvolume analysis of the isothermal compressibility for the TIP4P/2005 water model, and discuss the influence of reservoir size effects on the analysis. Conclusions are formulated in Sec. 7.

2 Grand-canonical small systems, as developed by Hill

Hill's development of thermodynamics for small systems is based on the idea that thermodynamics is valid for a large ensemble of $\mathscr{N}$ independent replicas of the small system. We are free to choose the environmental variables of the small system. Unlike in macroscopic thermodynamics, the properties of small systems depend on this choice[2]. Consider in particular an ensemble constructed by taking $\mathscr{N}$ independent, distinguishable, replicas of a one-component small system characterized by the temperature, the volume and the chemical potential (T, V, μ). The ensemble of replicas follows the laws of macroscopic thermodynamic systems when $\mathscr{N}$ is large enough, and the Gibbs relation is given by

$$dU_t^{GC} = TdS_t^{GC} - p^{GC}\mathscr{N}dV + \mu dN_t^{GC} + X^{GC}d\mathscr{N} \qquad (1)$$

The so-called replica energy of an ensemble member is given by

$$X^{GC}(T,V,\mu) \equiv \left(\frac{\partial U_t^{GC}}{\partial \mathscr{N}} \right)_{S_t,V,N_t} \qquad (2)$$

where the superscript GC specifies that the variables are functions of the environmental variables of the grand-canonical ensemble (T,V,μ). The subscript t denotes properties of the full ensemble. The replica energy, X^{GC}, can be interpreted as the work $-\hat{p}V$ required to increase the volume of the ensemble by adding one ensemble member, keeping S_t^{GC}, V, and S_t^{GC} constant, while $p^{GC}\mathscr{N}dV$ is the work required to increase the volume of the ensemble by increasing the volume of each member. The variable $\hat{p}$ is therefore called the *integral* pressure and is only equal to the *differential* pressure p in the thermodynamic limit. Using Euler's theorem of homogeneous functions we integrate Eq. (1) holding T,V,μ and X^{GC} constant to obtain

$$U_t^{GC}(T,V,\mu,\mathscr{N}) = TS_t^{GC}(T,V,\mu,\mathscr{N})$$
$$+ \mu N_t^{GC}(T,V,\mu,\mathscr{N}) - \hat{p}(T,V,\mu)V\mathscr{N} \qquad (3)$$

where we have used the definition $X^{GC} \equiv -\hat{p}V$. The ensemble av-

erages of internal energy, particle number, and entropy are given by

$$U_t^{GC}(T,V,\mu,\mathcal{N}) \equiv \mathcal{N}U^{GC}(T,V,\mu)$$

$$N_t^{GC}(T,V,\mu,\mathcal{N}) \equiv \mathcal{N}N^{GC}(T,V,\mu) \qquad (4)$$

$$S_t^{GC}(T,V,\mu,\mathcal{N}) \equiv \mathcal{N}S^{GC}(T,V,\mu)$$

While U^{GC} and N^{GC} fluctuate because the small systems are open, the entropy S^{GC} does not, and is the same for each ensemble member [2]. Substituting the relations in Eq. (4) into Eq. (3) we can write the average internal energy of a single small system as

$$U^{GC}(T,V,\mu) = TS^{GC}(T,V,\mu) + \mu N^{GC}(T,V,\mu) - \hat{p}(T,V,\mu)V \quad (5)$$

or alternatively

$$U^{GC} = TS^{GC} - p^{GC}V + \mu N^{GC} + (p^{GC} - \hat{p})V \qquad (6)$$

where we have, for ease of notation omitted, the dependencies of each variable. For a macroscopic system, where the integral pressure and differential pressure are equal, the correction term $(p^{GC} - \hat{p})V$ becomes zero, and we are left with the classical thermodynamic relation. For the small system enthalpy Eq. (5) gives

$$\hat{H}^{GC} \equiv U^{GC} + \hat{p}V = TS^{GC} + \mu N^{GC} \qquad (7)$$

The small system enthalpy differ from the enthalpy in the thermodynamic limit, through the use of $\hat{p}$ rather than p. We obtain the Gibbs relation for the small system by inserting the relations in Eq. (4) into Eq. (1), using $X^{GC} \equiv -\hat{p}V$ and Eq. (5)

$$dU^{GC} = TdS^{GC} - p^{GC}dV + \mu dN^{GC} \qquad (8)$$

By differentiating Eq. (5) and combining the result with Eq. (8) the Gibbs-Duhem like equation becomes

$$d(\hat{p}V) = S^{GC}dT + p^{GC}dV + N^{GC}d\mu \qquad (9)$$

From this we derive the expressions which are particular for a small system

$$S^{GC}(T,V,\mu) = \left(\frac{\partial \hat{p}V}{\partial T}\right)_{V,\mu}$$

$$p^{GC}(T,V,\mu) = \left(\frac{\partial \hat{p}V}{\partial V}\right)_{T,\mu} \qquad (10)$$

$$N^{GC}(T,V,\mu) = \left(\frac{\partial \hat{p}V}{\partial \mu}\right)_{T,V}$$

We see that as long as the systems are so small that the integral pressure $\hat{p}$ depends on the volume, the properties S^{GC}, p^{GC}, and N^{GC} are different from those of a large system. For large values

of V the integral pressure becomes independent of V, and one finds $p^{GC} = \hat{p}$. In that case Eq. (9) gives the usual Gibbs-Duhem equation. The information presented in this section gives us a basic understanding of the framework developed by Hill that allows us to consistently handle the thermodynamics of small systems. The last relations are needed to recover expressions for surface thermodynamics.

3 The surface contribution satisfies Gibbs' thermodynamics for flat surfaces

A property that is *extensive* in the sense of Hadwigers theorem [10] can, as a first order approximation, be written as the sum of contributions; one proportional to the volume and one to the surface area

$$a(T,V,\mu) = \frac{A(T,V,\mu)}{V} = a^{\infty}(T,\mu) + \frac{\Omega}{V}a^s(T,\mu) \qquad (11)$$

Here $a(T,V,\mu)$ is the density of A, a^{∞} and a^s are the volume and surface contributions of a respectively, Ω is the surface area, and V is the volume. By using Eq. (11), we can rewrite Eq. (8) in terms of separate contributions from the volume and the surface

$$d(u^{\infty}V) = Td(s^{\infty}V) + \mu d(n^{\infty}V) - p^{\infty}dV \qquad (12)$$

$$d(u^s\Omega) = Td(s^s\Omega) + \mu d(n^s\Omega) - p^s\frac{\Omega}{V}dV \qquad (13)$$

Superscript *GC* has now been omitted. We see that Eq. (12) is the classical thermodynamic description of a one-component homogeneous system. We now continue to develop the surface contribution. From our definitions $L \equiv V^{1/3}$ and $\Omega/V \equiv c_s/L$ we have

$$\left(\frac{\partial \Omega}{\partial V}\right)_{T,\mu} = \left(\frac{\partial \Omega}{\partial L}\right)_{T,\mu}\left(\frac{\partial L}{\partial V}\right)_{T,\mu} = \frac{2c_sL}{3L^2} = \frac{2}{3}\frac{c_s}{L} = \frac{2}{3}\frac{\Omega}{V}$$

$$\Rightarrow \frac{\Omega}{V}dV = \frac{3}{2}d\Omega \qquad (14)$$

Substituting the last expression into Eq. (13) gives the Gibbs equation for the surface

$$d(u^s\Omega) = Td(s^s\Omega) + \mu d(n^s\Omega) - \frac{3}{2}p^sd\Omega \qquad (15)$$

By using the relation between the integral pressure $\hat{p}$ and the differential pressure p in Eq. (10), and separating the contributions

according to Eq. (11), we obtain

$$p(T,V,\mu) = \left(\frac{\partial \hat{p}(T,V,\mu)V}{\partial V} \right)_{T,\mu}$$

$$= \left(\frac{\partial \hat{p}^{\infty}(T,\mu)V}{\partial V} \right)_{T,\mu} + \left(\frac{\partial \hat{p}^{s}(T,\mu)\Omega}{\partial V} \right)_{T,\mu}$$

$$= \hat{p}^{\infty}(T,\mu) + \hat{p}^{s}(T,\mu) \left(\frac{\partial \Omega}{\partial V} \right)_{T,\mu} \qquad (16)$$

$$= \hat{p}^{\infty}(T,\mu) + \frac{2}{3}\frac{c_s}{L}\hat{p}^{s}(T,\mu)$$

By multiplying with the volume, we can write pV as

$$p(T,V,\mu)V = \hat{p}^{\infty}(T,\mu)V + \frac{2}{3}\Omega\hat{p}^{s}(T,\mu)$$

$$= p^{\infty}(T,\mu)V + p^{s}(T,\mu)\Omega \qquad (17)$$

where

$$p^{\infty} = \hat{p}^{\infty} \quad \text{and} \quad p^{s} = \frac{2}{3}\hat{p}^{s} \qquad (18)$$

The first equality is an identity. The surface pressures p^{s} and $\hat{p}^{s}$ are proportional to one another. They can be replaced by the surface tension according to

$$\gamma(T,\mu) \equiv -\hat{p}^{s}(T,\mu) = -\frac{3}{2}p^{s}(T,\mu) \qquad (19)$$

The Gibbs-Duhem type equation for the small system surface is

$$d(\hat{p}^{s}\Omega) = S^{s}dT + N^{s}d\mu + \frac{3}{2}p^{s}d\Omega \qquad (20)$$

By substituting the pressures according to Eq. (19) and dividing by the surface area, we arrive at the standard Gibbs-Duhem equation for the surface

$$d\gamma(T,\mu) = -s^{s}(T,\mu)dT - n^{s}(T,\mu)d\mu \qquad (21)$$

We see that when we follow Hill's small system analysis and consider the volume and surface contributions as separate contributions, we obtain the classical thermodynamic equation for a homogeneous system for the volume contribution, and the Gibbs surface relation for the surface contribution. This shows us that Hill's description agrees with classical thermodynamics, and that the small system surface satisfies Gibbs thermodynamics when the surface is flat. We can therefore study the thermodynamic properties of the surface using Hill's thermodynamics for small systems.

4 Volume and surface contributions of thermodynamic functions from fluctuations

Having established the thermodynamic framework for the volume and surface contributions to various thermodynamic properties,

we now present a route to efficiently obtain such contributions from molecular dynamics simulations. The link between the probability distributions of statistical mechanics and Hill's thermodynamics of small systems in the grand-canonical ensemble is given by[2]

$$\hat{p}(T,V,\mu)V = k_B T \ln \Xi(T,V,\mu) \qquad (22)$$

where Ξ is the grand-canonical partition function. From derivatives of the partition function we can obtain probability distribution moments, of which the second moments quantify the fluctuations of particle number and energy. According to Eq. (22) these fluctuations are related to derivatives of $\hat{p}(T,V,\mu)V$. Taking the second derivative of Eq. (22) with respect to the chemical potential and substituting the left hand side according to Eq. (10), we have

$$k_B T \left(\frac{\partial N}{\partial \mu} \right)_{T,V} = (k_B T)^2 \left(\frac{\partial^2 \ln \Xi(T,V,\mu)}{\partial \mu^2} \right)_{T,V}$$

$$= \langle N^2 \rangle - \langle N \rangle^2 \qquad (23)$$

In the thermodynamic limit the thermodynamic factor is defined by

$$\Gamma \equiv \frac{N}{k_B T} \left(\frac{\partial \mu}{\partial N} \right)_{T,V} \qquad (24)$$

Using Eq. (23) we therefore define

$$\nu \equiv \frac{k_B T}{V} \left(\frac{\partial N}{\partial \mu} \right)_{T,V} = \frac{\langle N^2 \rangle - \langle N \rangle^2}{V} = \nu^{\infty} + \frac{\Omega}{V}\nu^{s} \qquad (25)$$

Note that $\nu/n \neq 1/\Gamma$, where $n \equiv \langle N \rangle / V$ is the particle density. By expanding this according to Eq. (11), we can relate the volume and surface terms of ν to the particle fluctuation in the grand-canonical ensemble in the last equality. We use that N, U, $(\partial N/\partial \mu)_{T,V}$ and $(\partial N/\partial \mu)_{T,V}$ are all extensive in the sense of Hadwigers theorem[10]. The derivative of the internal energy density, $u \equiv \langle U \rangle / V$, with respect to the chemical potential, μ, in terms of the fluctuations of energy and particles is

$$k_B T \left(\frac{\partial u}{\partial \mu} \right)_{T,V} = k_B T \left(\frac{\partial u}{\partial \mu} \right)_{T,V}^{\infty} + k_B T \frac{\Omega}{V} \left(\frac{\partial u}{\partial \mu} \right)_{T,V}^{s}$$

$$= \frac{\langle UN \rangle - \langle U \rangle \langle N \rangle}{V} \qquad (26)$$

These equations will be applied for analyses of small volumes of water below.

The isothermal compressibility

The quantity ν enters the expression for the isothermal compressibility, κ_T, of the liquid. This is a quantity of practical interest. The

definition gives

$$\kappa_T = \frac{V}{N^2}\left(\frac{\partial N}{\partial \mu}\right)_{T,V} = -\frac{V}{N^2}\left(\frac{\partial^2 \hat{p}V}{\partial \mu^2}\right)_{T,V} = \frac{1}{n^2 k_B T}v$$

$$= \frac{1}{n^2 k_B T}\frac{\langle N^2\rangle - \langle N\rangle^2}{V} \tag{27}$$

By introducing Eq. (25) we obtain

$$\kappa_T = \frac{1}{k_B T}\left[v^\infty + \frac{\Omega}{V}v^s\right]\bigg/\left[n^\infty + \frac{\Omega}{V}n^s\right]^2 \tag{28}$$

The isothermal compressibility is not an extensive quantity in the sense of Hadwiger's theorem [10] and can therefore in general not be written as the sum of a volume and a surface contribution. For the special case that $n^s = 0$, relevant for the small systems considered in this and earlier papers, however, the above equation reduces to

$$\kappa_T = \frac{1}{(n^\infty)^2 k_B T}\left[v^\infty + \frac{\Omega}{V}v^s\right] = \kappa_T^\infty + \frac{\Omega}{V}\kappa_T^s \tag{29}$$

So in the special case that $n^s = 0$, the isothermal compressibility can be written as the sum of a volume and a surface contribution:

$$\kappa_T^\infty = \frac{1}{n^2 k_B T}v^\infty \quad \text{and} \quad \kappa_T^s = \frac{1}{n^2 k_B T}v^s \tag{30}$$

where $n = n^\infty$.

Kirkwood-Buff integrals are often used to express thermodynamic properties [16]. The isothermal compressibility in terms of a Kirkwood-Buff integral is

$$\kappa_T = \frac{1}{n k_B T}\left(1 + nG(R)\right) = \frac{1}{n k_B T}\left(1 + nG^\infty + n\frac{\Omega}{V}G^s\right) \tag{31}$$

For the special case that $n^s = 0$ it follows that

$$\kappa_T^\infty = \frac{1}{n k_B T}\left(1 + nG^\infty\right) \quad \text{and} \quad \kappa_T^s = \frac{1}{k_B T}G^s \tag{32}$$

In these equations, the integral, $G(R)$, is defined for a sphere of radius R, see e.g. [7]

$$G(R) = 4\pi \int_0^{2R} h(r)r^2\left(1 - \frac{3r}{4R} + \frac{r^3}{16R^3}\right)dr \tag{33}$$

Here $h(r) \equiv g(r) - 1$, where $g(r)$ is the pair correlation function of an infinitely large system. The quantity $h(r)$ does not converge to 0 for $r \to \infty$ in a closed system [16]. A positive excess density at a given distance from the particle center, affects the density in the rest of the system. This can be taken into account by correcting the pair correlation function [8].

The partial enthalpy and partial internal energy

Further remarks on fluctuating properties in the grand-canonical ensemble can be made for the sake of completeness. From the definition of the enthalpy of a small system, $\hat{H} \equiv U + \hat{p}V$, we can obtain the derivative of the enthalpy density, $\hat{h}$, with respect to the chemical potential, μ, for small systems by the combination

$$\left(\frac{\partial \hat{h}}{\partial \mu}\right)_{T,V} = \left(\frac{\partial u}{\partial \mu}\right)_{T,V} + \left(\frac{\partial \hat{p}}{\partial \mu}\right)_{T,V} = \left(\frac{\partial u}{\partial \mu}\right)_{T,V} + n \tag{34}$$

It follows that

$$\left(\frac{\partial \hat{h}}{\partial \mu}\right)_{T,V,\mu}^\infty = \left(\frac{\partial u}{\partial \mu}\right)_{T,V}^\infty + n^\infty$$

$$\left(\frac{\partial \hat{h}}{\partial \mu}\right)_{T,V,\mu}^s = \left(\frac{\partial u}{\partial \mu}\right)_{T,V}^s + n^s \tag{35}$$

The combination of Eq. (25) and Eq. (26) as well as $n = \langle N\rangle/V$ is sufficient to obtain v/n, partial internal energy, and partial enthalpy according to Eqs. (36),(37) and (38) respectively.

$$\frac{v}{n} = \left[v^\infty + \frac{\Omega}{V}v^s\right]\bigg/\left[n^\infty + \frac{\Omega}{V}n^s\right]$$

$$= \frac{\langle N^2\rangle - \langle N\rangle^2}{\langle N\rangle} \tag{36}$$

$$\left(\frac{\partial \langle U\rangle}{\partial \langle N\rangle}\right)_{T,V,\mu} = k_B T\left[\left(\frac{\partial u}{\partial \mu}\right)_{T,V}^\infty + \frac{\Omega}{V}\left(\frac{\partial u}{\partial \mu}\right)_{T,V}^s\right]$$

$$\bigg/\left[v^\infty + \frac{\Omega}{V}v^s\right] = \frac{\langle UN\rangle - \langle U\rangle\langle N\rangle}{\langle N^2\rangle - \langle N\rangle^2} \tag{37}$$

$$\left(\frac{\partial \langle \hat{H}\rangle}{\partial \langle N\rangle}\right)_{T,V,\mu} = k_B T\left[\left(\frac{\partial u}{\partial \mu}\right)_{T,V}^\infty + n^\infty + \frac{\Omega}{V}\left(\left(\frac{\partial u}{\partial \mu}\right)_{T,V}^s + n^s\right)\right]$$

$$\bigg/\left[v^\infty + \frac{\Omega}{V}v^s\right] = \frac{\langle UN\rangle - \langle U\rangle\langle N\rangle + \langle N\rangle k_B T}{\langle N^2\rangle - \langle N\rangle^2} \tag{38}$$

These properties are not extensive in the sense of Hadwigers theorem [10].

## On the importance of extrapolating extensive properties

It was noted in the previous section that the proper quantities to expand in volume and surface contributions are extensive. The reason for this is that Hadwiger's theorem [10] applies to such properties only. The quantities in Eqs. (25) and (26) as well as n and u are proper quantities in this respect.

We have used Eq. (11) and given them as the sum of a volume and a surface contribution. The surface terms depend on the
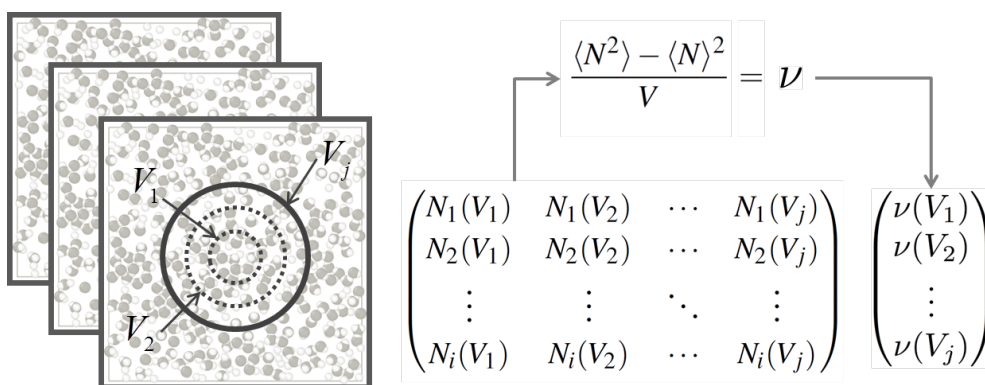
Fig. 1 Constructing grand-canonical ensembles of small systems. Left: illustration of the sampling of small systems in a closed reservoir, showing three configurations from the simulation trajectory. Right: To use the fluctuation equation with the collection of samples for each subvolume size $V = L^3$, gives ν as a function of size.

Table 1 Values for the shape dependent coefficient $c_s \equiv \Omega/V^{2/3}$. The sidelength of each prism is given by a, and the radius of the sphere is given by R.

Shape	c_s		
	$c_s = \dfrac{\Omega}{V^{2/3}} = \dfrac{\sqrt{3}a^2}{(a^3/6\sqrt{2})^{2/3}}$	$\approx$	7.2
	$c_s = \dfrac{\Omega}{V^{2/3}} = \dfrac{6a^2}{(a^3)^{2/3}}$	$=$	6
	$c_s = \dfrac{\Omega}{V^{2/3}} = \dfrac{3\sqrt{25+10\sqrt{5}}a^2}{[(15+7\sqrt{5})a^3/4]^{2/3}}$	$\approx$	5.3
	$c_s = \dfrac{\Omega}{V^{2/3}} = \dfrac{4\pi R^2}{(4\pi R^3/3)^{2/3}}$	$\approx$	4.8

temperature and the chemical potential, but are independent of the size. In Eqs. (36), (37) and (38) we consider combinations of these quantities using non-linear operations such as division. These combinations are not extensive quantities, however, in the sense of Hadwiger's theorem. As a consequence, these quantities can not be written as the sum of volume and surface contributions. The equations show that they are more complicated combinations of the volume and surface contributions.

Small system properties can be extrapolated to the thermodynamic limit using the scaling law, only when the properties are extensive in the sense of Hadwiger's theorem. Only then, can we substitute resulting thermodynamic limit values in Eqs. (36), (37) and (38) to obtain the thermodynamic limit values of the combinations.

For subvolume diameters below the molecular diameter, N is

either 0 or 1. The limits of ν, $k_B T (\partial u/\partial \mu)_{T,V}$ and $k_B T (\partial \hat{h}/\partial \mu)_{T,V}$ then follow

$$\lim_{V \to 0} \nu = \lim_{V \to 0} \frac{\langle N^2 \rangle - \langle N \rangle^2}{V}$$

$$= \frac{\langle N \rangle - \langle N \rangle^2}{V} \approx \frac{\langle N \rangle}{V} = n$$

$$\lim_{V \to 0} k_B T \left(\frac{\partial u}{\partial \mu} \right)_{T,V} = \lim_{V \to 0} \frac{\langle UN \rangle - \langle U \rangle \langle N \rangle}{V} \qquad (39)$$

$$= \frac{\langle U \rangle - \langle U \rangle \langle N \rangle}{V} \approx \frac{\langle U \rangle}{V} = u$$

$$\lim_{V \to 0} k_B T \left(\frac{\partial \hat{h}}{\partial \mu} \right)_{T,V} = u + n k_B T$$

where we used that U is also zero when $N = 0$. These expressions are the same as for an ideal gas.

For the small systems considered here and earlier[5–7,9], we find that $n^s = 0$. As we can see in Eqs. (28) and (36), this implies that the terms containing Ω/V in the denominators disappear. For this special case it is then possible to write the combinations as sums of volume and surface contributions. One may even write $\nu/n = 1/\Gamma$ in this case. While this is convenient, one should still remember that the Small System Method only applies to quantities which are extensive in the sense of Hadwiger's theorem. Note that $n^s = 0$ does not imply that ν^s is equal to zero.

5 Simulation details

Methodology

The molecular dynamics simulations reported here were done using the open source code LAMMPS (version 14 May 2016)[17]. Input files were adapted from the notes made available at http://www.orsi.sems.qmul.ac.uk/downloads.html[18]. The reser-

Table 2 Simulation parameters for the water models. The units are $mass \cdot g^{-1} \cdot mol$, $length \cdot \text{Å}^{-1}$, $charge \cdot e^{-1}$, $energy \cdot kJ^{-1} \cdot mol$ and $angle \cdot degree$ [12–15]

	SPC/E	TIP3PEw	TIP4PEw	TIP4P/2005
O_{mass}	15.9994	15.9994	15.9994	15.9994
H_{mass}	1.008	1.008	1.008	1.008
O_{charge}	-0.8476	-0.830	-1.0484	-1.1128
H_{charge}	0.4238	0.415	0.5242	0.5564
$OH_{bond\,length}$	1.0	0.9572	0.9572	0.9572
HOH_{angle}	109.47	104.52	104.52	104.52
$OO\varepsilon_{LJ}$	0.6498	0.4268	0.6809	0.7749
$OO\sigma_{LJ}$	3.166	3.188	3.16435	3.1589
$OM_{distance}$	n/a	n/a	0.1250	0.1546
r_c	8.5	8.5	8.5	8.5

voir referred to in the Small System Method was represented by a cubic simulation box with periodic boundary conditions. The small systems were represented by volumetric selections within the reservoir. For instance, a spherical small system with radius R, centered at $p_c = (x_c, y_c, z_c)$, was defined to be the set of all points $p_s = (x_s, y_s, z_s)$ satisfying $(x_s - x_c)^2 + (y_s - y_c)^2 + (z_s - z_c)^2 \leq R^2$. The reservoir size and number of molecules were set to $L_x = L_y = L_z = 62\,\text{Å}$ and $N = 8000$ for the small system shape comparison in Figures 2 and 3, and for the comparison of water models in Figure 4. When calculating the isothermal compressibility we increased the system size to $L_x = L_y = L_z = 124\,\text{Å}$ with $N = 64000$ water molecules in order to minimize the finite reservoir size effect. The simulations comparing different reservoir sizes in Figure 6 were performed at the same density and pressure with the reservoir sizes ranging from 18 to 124 Å.

All simulations were performed with a time step of 1 fs, and the initial configuration was created by replicating a single water molecule across a cubic lattice with subsequent equilibration for 200 ps in the isothermal-isobaric ensemble with thermostat and barostat relaxation times of 0.1 ps and 1 ps respectively. The production runs were performed in the canonical ensemble for 10^6 fs with a thermostat relaxation time of 0.1 ps. The Nosé-Hoover thermostat and barostat were used as implemented in LAMMPS [19–22].

We obtained $\langle N^2 \rangle$ and $\langle N \rangle^2$ for each small system volume V from the simulation trajectory using the Small System Method [9]. The system configuration and total energy per molecule were stored from the trajectory every 100 fs over a total of 10^6 fs. For each configuration and volume V we sampled the particle count in 500 randomly positioned small systems, accumulating a total of $5 \cdot 10^6$ samples for each V for statistical analysis. The samples were used to calculate v and $k_B T (\partial u / \partial \mu)_{T,V}$ according to Eqs. (25) and (26). The process is illustrated in Figure 1.

The finite volume Kirkwood-Buff integrals in Figure 5 were calculated from the pair correlation function of the system up to half of the reservoir size [7]. The pair correlation function was taken from the same trajectory as the Small System Method, with the same sampling interval.

Case studies

Four different small system-shapes were investigated, see Table 1. The shapes were chosen to include the largest area to volume ratio possible for a regular polygonal prism (tetrahedron), and the smallest area to volume ratio limit (sphere). The table shows the shape dependent coefficient $c^s \equiv \Omega/(V^{2/3})$, which for equal volume gives the relative magnitude of the surface area for the different shapes. We used the SPC/E [12] model to examine the general trends related to the shape, because it has a lower computational cost compare to the 4-site models of water. When comparing thermodynamic properties calculated according to the procedures described above, we used the water models SPC/E, TIP3PEw [13], TIP4PEw [14] and TIP4P/2005 [15]. The TIP4P/2005 model was selected for the calculation of the isothermal compressibility because it describes the behavior of this property for water very well. The pressure range for the compressibility simulations included a negative pressure simply to get a point on both sides of 1 bar.

Interaction models

We used the SPC/E [12], TIP3PEw [13], TIP4PEw [14] and TIP4P/2005 [15] water models in our simulations. The specific parameters for each model are summarized in Table 2. For all models, the intermolecular interactions between oxygen atoms i and j were given by the Lennard-Jones (LJ) potential

$$u_{LJ}(r_{ij}) = 4\varepsilon \left[\left(\frac{\sigma}{r_{ij}} \right)^{12} - \left(\frac{\sigma}{r_{ij}} \right)^6 \right], \quad r_{ij} < r_c \qquad (40)$$

where ε is the potential well depth, σ is the separation at which the potential is zero, and r_{ij} is the distance of separation between the particle centers. Long-range corrections for the LJ potential were applied to the energy and the pressure, except for TIP3PEw, consistent with the reference. Long-range Coulombic interactions were computed according to the particle-particle particle-mesh (PPPM) method [23]. This was also done for the SPC/E model, which means it is a variation of the original model. Bond lengths and angles were reset to their equilibrium values each timestep using the SHAKE algorithm [24].

Table 3 Molecular dynamics simulation results for volume and surface contributions of selected thermodynamic properties. The results are averages of 5 simulations with different initial velocities, and the uncertainties with 95% confidence are below 2% for v^∞ and $k_B T (\partial u/\partial \mu)_{T,V}^\infty$, and below 0.5% for v^s and $k_B T (\partial u/\partial \mu)_{T,\Omega}^s$. Numerical subscripts indicate the accuracy of the last decimal e.g. 32.4_4 means 32.4 ± 0.4.

	SPC/E	TIP3PEw	TIP4PEw	TIP4P/2005
T/K	298	298	298	298
$n^\infty \cdot nm^3$	33.3	33.3	33.3	33.3
$n^s \cdot nm^2$	0.0	0.0	0.0	0.0
$u^\infty \cdot MJ^{-1} \cdot dm^3$	-2.16	-1.88	-2.14	-2.22
$u^s \cdot J^{-1} \cdot m^2$	0.0	0.0	0.0	0.0
$v^\infty \cdot nm^3$	1.99_4	2.50_3	1.99_4	1.94_1
$v^s \cdot nm^2$	0.716_5	0.727_5	0.710_5	0.703_3
$k_B T \left(\frac{\partial u}{\partial \mu}\right)_{T,V}^\infty \cdot MJ^{-1} \cdot dm^3$	-0.146_3	-0.171_3	-0.139_3	-0.138_1
$k_B T \left(\frac{\partial u}{\partial \mu}\right)_{T,\Omega}^s \cdot J^{-1} \cdot m^2$	-0.0457_3	-0.0399_4	-0.0454_4	-0.0465_3
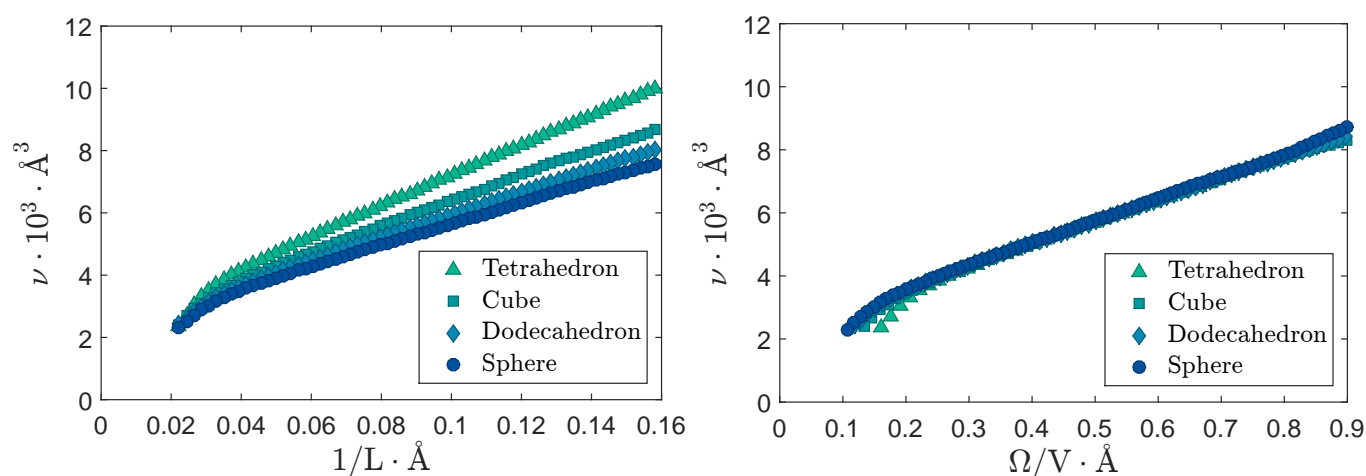
Fig. 2 How the small system shape contributes to the slope of v. Molecular dynamics simulations of water using the SPC/E model [12] at a density $\rho = 1\,g\,cm^{-3}$ and a temperature $T = 298$ K. Left: v calculated from Eq. (25) for four different small system shapes ranging from the simplest regular polygonal prism (tetrahedron), to a sphere. The volumes are given by the characteristic length $L = V^{1/3}$, indicating that each shape has the same volume for a given abscissa, the surface area however is different. Right: the curves corresponding to those in the left panel with the shape dependent contribution to the slope corrected.

6   Results

Zero surface excess density and surface internal energy density

Before we proceed to discuss the new results, we establish the validity of the basic assumption behind the separation of bulk and surface contributions to κ_T and v/n; that is the requirement $n^s = 0$. Within the numerical accuracy of the simulations, we confirm in all cases that $n^s = 0$ for all water models studied (cf. Table 3), as expected. This means that there is no tendency for the particles to accumulate at the subvolume surface.

Nevertheless, the statistics for an open subvolume are different from that of a volume with periodic boundaries, and this is related to a difference in entropy between the two. The correlations be-

tween particles close to the subvolume surface are different from the correlations far from the surface. This will show in the fluctuations of the number of particles in the subvolume. The quantity v is calculated from such fluctuations, and can be used to find the compressibility of the liquid. While v can have non-zero volume and surface contributions, for a property like n^s these correlations do not contribute. The same reasoning applies to the fluctuations in energy and the quantity u^s which is also zero (cf. Table 3). As a result from the simulations, we find for all the water models

$$n = n^\infty + \frac{\Omega}{V} n^s = n^\infty$$

$$u = u^\infty + \frac{\Omega}{V} u^s = u^\infty$$

(41)

This establishes the basis for the validity of the scaling laws for
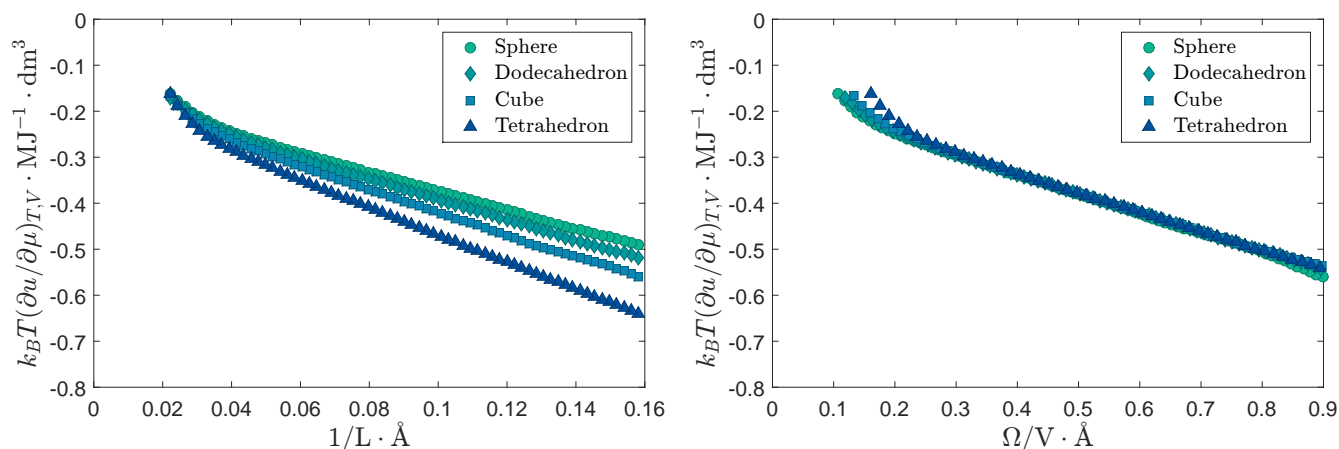
Fig. 3 How the small system shape contributes to the slope of $k_B T (\partial u / \partial \mu)_{T,V}$. Molecular dynamics simulation of water using the SPC/E model [12] at a density of $\rho = 1\,\mathrm{g\,cm^{-3}}$ and a temperature of $298\,\mathrm{K}$. Left: $k_B T (\partial u / \partial \mu)_{T,V}$ calculated from Eq. (26) for four different small system shapes ranging from the simplest regular polygonal prism (tetrahedron), to a sphere. The volumes are given by the characteristic length $L = V^{1/3}$, indicating that each shape has the same volume for a given point, the surface area however is different. Right: the curves corresponding to those in the left panel with the shape dependent contribution to the slope removed.

κ_T and v/n in Eqs. (29) and (36). We note that for $n^s = 0$ one may write $v/n = 1/\Gamma$.

A scaling law for shapes and sizes

Figure 2 (left panel) shows v vs. $1/L = V^{-1/3}$ for the four different small system shapes we investigated. The right panel of this figure shows v vs. Ω/V. We see that the slopes of the curves in the left panel depend on the shape of the small system. There is a systematically increasing slope from spherical shape to tetrahedral shape. This is reflected in the different area to volume ratios of the shapes, as indicated by the shape dependent coefficient c_s in Table 1.

When we plot against $1/L$, the volumes of the different shapes are the same when L is given. The surface areas differ, however. As a consequence, the linear region of the curve, which we associate with the surface contribution, depends on the subvolume shape. The thermodynamic limit value, however, must be independent of the shape. This is documented by the left panel of the figure: All curves extrapolate to the same point when $1/L \to 0$.

It is possible to correct for the shape dependence, by plotting v as a function of Ω/V. This produces the plots in Figure 2 (right panel). Here all curves for the shapes in the left panel collapse on the same curve, as they obtain the same slope and limit values. This confirms that the surface contribution is intrinsic and proportional to the area to volume ratio, as predicted by Eq. (11). It also enables us to predict surface contributions, independent of shape, once the surface to volume ratio is known.

Figure 3 shows the shape dependence of the energy-density correlations, cf. Eq. (26). Similar to Figure 2, the curves in the left panel have different slopes depending on the small system

shape, and the limit values are the same. The curves in the right panel are independent of the shape. The results are consistent with 2, confirming that also the energy-density correlations can be represented by Eq. (11).

The characteristic slope and ordinate of the properties for the four water models are listed in Table 3. They will be discussed below. The scaling law applies to a particular region which will also be discussed below.

Scaling law - limits of validity

For the largest of the embedded small systems, when $1/L \to 0$, we observe deviations from linear behavior (cf. Figure 2). The effect becomes significant at the same volume for each shape, as opposed to being dependent on the area to volume ratio. This confirms that the reservoir is the origin of this effect.

The reason is that the simulation box is not functioning properly as a grand-canonical reservoir for the small systems when they approach the size of the reservoir [9]. This can be understood from the following: For closed systems, a density change in a subvolume can not occur without a corresponding density change in the reservoir. The significance of the correlation between the two densities increases with the volume fraction of the subvolume in the reservoir. At the extreme where the fraction is unity, all the available particles are contained within the subvolume at all times, and the fluctuation becomes zero. As a consequence, we observe that the curves drop off as the small system approaches the reservoir size.

A formula for the finite reservoir effect was suggested [9], and a method for implicitly accounting for it [6] was proposed. We support the explanation of the reservoir effect above, and further de-
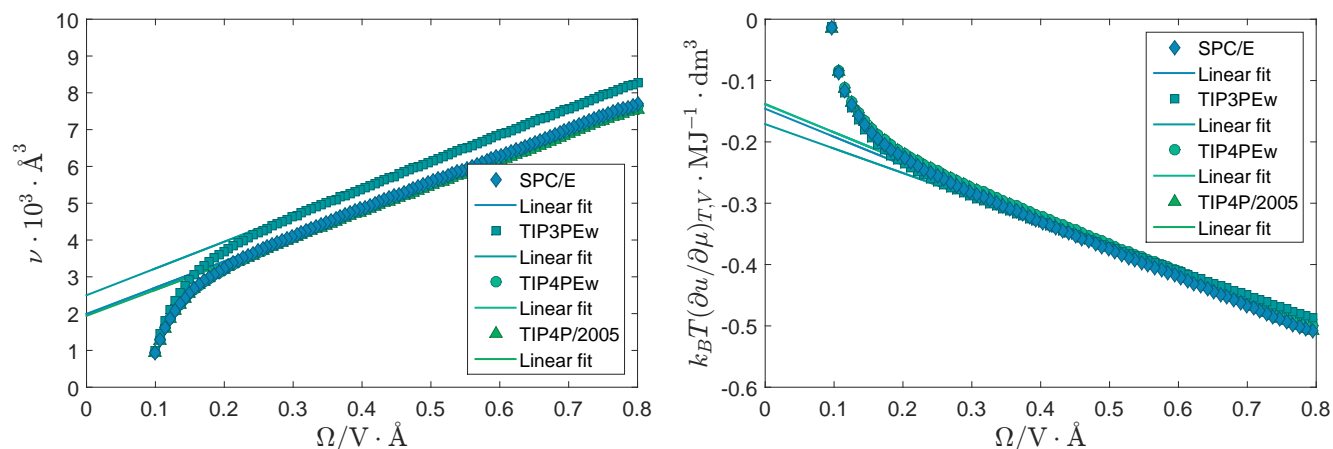
Fig. 4 Size effect of thermodynamic properties, independent of system shape, for a selection of common water models. The T,V,μ ensembles for each water model were obtained from MD simulations in a (T,V,N) reservoir at a density of $\rho = 1\,\mathrm{g\,cm^{-3}}$ and a temperature of $298\,\mathrm{K}$. Left: v calculated from Eq. (25) for different small system sizes characterized by $L = V^{1/3}$. Right: $k_B T (\partial u / \partial \mu)_{T,V}$ calculated using Eq. (26) for the same ensembles as in the left panel.

velop the previous work by explicitly obtaining the finite reservoir contributions to the volume and surface terms here. Assuming the effect is a function of the volume fraction of the subvolume in the reservoir only, we can write

$$v = v^\infty + \frac{\Omega}{V} v^s + v^r \frac{V}{V^r} \tag{42}$$

where v^r is the contribution from the reservoir effect, and V^r is the reservoir volume. As described above, when the suvolume fraction V/V^r is unity we get

$$v^\infty + \frac{\Omega^r}{V^r} v^s + v^r = 0 \tag{43}$$

where Ω^r is the surface area of the reservoir. Solving for v^r and substituting v^r in Eq. (42) gives

$$v = \left[1 - \frac{V}{V^r}\right] v^\infty + \frac{\Omega}{V}\left[1 - \left(\frac{V}{V^r}\right)^{4/3}\right] v^s \tag{44}$$

When $V << V^r$ Eq. (44) reverts back to (25). Both the surface term and the volume term are affected by the finite reservoir volume and this leads to an underestimation of the value of v if the reservoir is not large enough.

For the smallest of the embedded small systems, there are higher order effects from edges, curvature and corners. These contributions result in deviations from linear behavior at the other end of the curve. In the limit where $1/L \to \infty$, the particle fluctuations and energy-density correlations are given by Eq (39). For more details the reader is referred to[9].

Sign of scaling law slope

The slope of the curves in Figure 2 (right panel) is positive, and this can be understood from the system properties. Earlier work on small systems for particles that interact with the purely repulsive Weeks-Chandler-Anderson potential[5] has also given a positive slope for v vs. $1/L$. This is different from Lennard-Jones particles results, which give a negative slope at low particle density ($\rho^* = 0.15$), and positive slope for higher particle density ($\rho^* = 0.6$). These observations suggest that repulsive interactions dominate at higher densities.

The positive slope for v can also be seen in terms of the increasing number of available configurations per volume when the subvolume becomes smaller. The second moment of the particle distribution increases as additional configurations made possible by the non-periodic boundary condition of the surface allow the particle number to fluctuate within a larger range. While the number of additional configurations increases with the surface area, the number of additional configurations per volume increases with Ω/V. This contributes to an increase of the second moment of the particle density distribution.

For low density Lennard-Jones particles, this contribution is compensated, for reasons that are not entirely clear to us, so that the slope of v becomes negative. However, the observations indicate that there is a balance between energetic and entropic effects.

Contributions to the compressibility from bulk and surface

Figure 4 and Table 3 shows our results for the four common water models. The surface and volume contributions to v and $k_B T (\partial u / \partial \mu)_{T,V}$ for each model are summarized in Table 3.
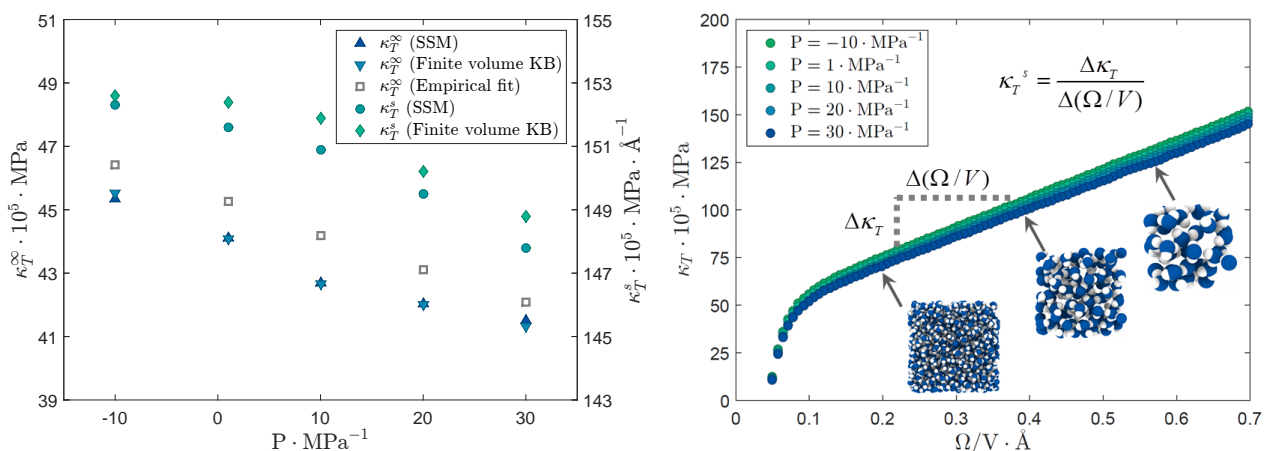
Fig. 5 Variation of isothermal compressibility volume and surface terms with pressure. The results are for the TIP4P/2005 water model at 298 K. Left: SSM was calculated from Eq. (29), finite volume KB was calculated from Eq. (32) and Eq. (33), and pressure-volume data was fitted using an empirical equation obtained from [25]. The left and right axes describe κ_T^∞ and κ_T^s respectively. Right: κ_T corresponding to the data in the left panel as a function of subvolume size. The molecular snapshot overlays are representative of the subvolume size for the curve region they point to.

All water models, except one, give approximately the same scaling law for the plots versus Ω/V. There are no significant variations in the surface contribution, v^s, between the models. Only the TIP3PEw model deviates from the other models' results for v^∞. At 298 K, for a number density of $n = 33.3$ nm^{-3}, the internal energy density varies from the lowest value -2.22 MJ·dm^{-3} for TIP4P/2005, to the highest value -1.88 MJ·dm^{-3} for TIP3PEw. In general, the TIP3PEw model stands out from the other models, but it is known in the literature that this can be the case for certain properties [26]. We relate the deviations we observe for TIP3PEw to the model's noticeably different local structure and molecular interaction parameters.

For instance, the Lennard-Jones parameter for the oxygen-oxygen iteraction ($OO_{\varepsilon_{LJ}}$) in Table 2 is approx. 30% lower than the other models, and the pair correlation function for TIP3PEw does not agree well with the experimental results for water. Important is that the more common models agree within the accuracy of the calculation.

It is also possible to obtain the same results using the more commonly known Kirkwood-Buff integrals. Figure 5 shows our results for the isothermal compressibility of TIP4P/2005 using both the Small System Method and the Kirkwood-Buff integrals. The left panel shows the volume and surface terms for pressures between -10 and 30 MPa, while the curves from which the terms were obtained are given in the right panel. We see that κ_T from both routes of calculation agree well for the pressures investigated here.

The volume terms, κ_T^∞, and the surface terms, κ_T^s, in Figure 5 are given in Table 4 with errors less than 5% and 2% respectively, with 95% confidence.

The calculation of κ_T from the Kirkwood-Buff integral is far

more sensitive to the value of G, than the corresponding calculation of κ_T from the Small System Method is sensitive to the value of v. According to Eq. (30), a 5 % variation in v^∞ corresponds to a 5 % variation in κ_T^∞. From Eq. (32), using representative values $\kappa_T = 45.6 \cdot 10^{-5}$ MPa^{-1}, $n = 0.0334$ Å^{-3}, and $G^\infty = -28.1$ Å^3, we find that the same 5 % variation in κ_T^∞ would require a variation in G^∞ of only 0.3 %. The thermodynamic limit value of

Table 4 Volume and surface terms for the isothermal compressibility of TIP4P/2005 [15] at $T = 298$ K and varying pressure. The values correspond to the data in Figure 5 (left panel). The volume terms, κ_T^∞, and the surface terms, κ_T^s, are given with estimated errors less than 5% and 2% respectively, with 95% confidence.

$P \cdot$ bar^{-1}	$\kappa_T^\infty \cdot 10^5 \cdot$ MPa	$\kappa_T^s \cdot 10^5 \cdot$ MPa $\cdot$ Å^{-1}
-100	45.3	152.3
1	44.1	151.6
100	42.7	150.9
200	42.0	149.5
300	41.5	147.8

κ_T for water is expected to be small because of the strong intermolecular interactions resulting in a relatively high density and thereby a low potential for compression. For TIP4P/2005 our results give $\kappa_T^\infty = (44.1 \pm 2.2) \cdot 10^{-5}$ MPa^{-1} at P = 1 bar, which within the statistical uncertainty agrees well with the experimental value [27], $45.3 \cdot 10^{-5}$ MPa^{-1}, and the value of TIP4P/2005 from [28], $(46.3 \pm 1.4) \cdot 10^{-5}$ MPa^{-1}. The fact that the comparison of bulk values makes sense, gives credibility to the new surface contributions. Comparing the two columns of Table 4, we find that the surface contributions are large, and will more than double the system's compressibility. The compressibility increases as the system becomes smaller.
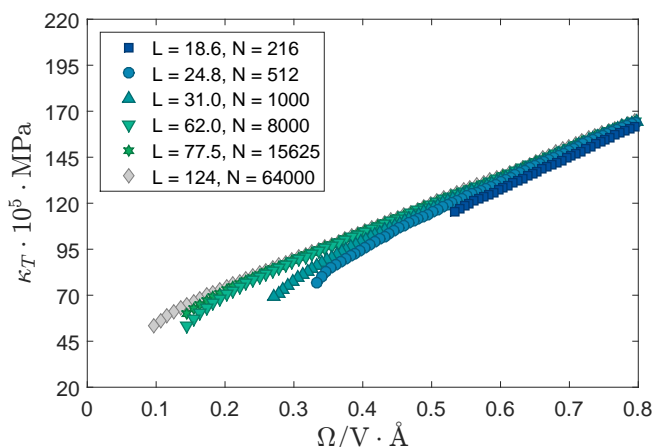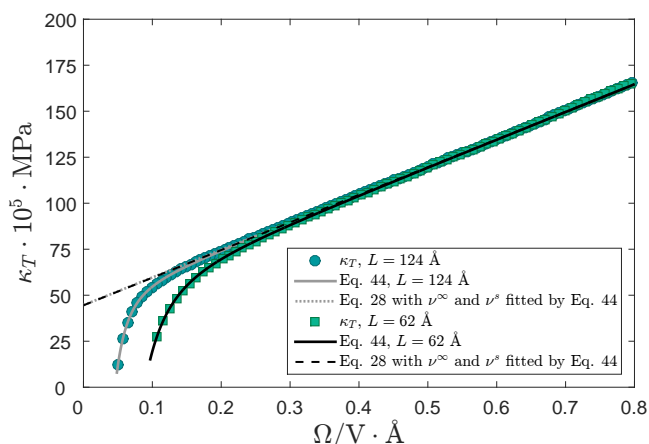
Fig. 6 Finite reservoir effect on subvolume analysis of isothermal compressibility for TIP4P/2005 at $P = 1$ bar and $T = 298$ K. The different reservoir sizes are indicated by the side length $\mathrm{L} \cdot \mathring{\mathrm{A}}^{-1}$, and the number of molecules N.

Fig. 7 Finite reservoir correction for subvolume analysis of isothermal compressibility for TIP4P/2005 at $P = 1$ bar and $T = 298$ K. The two reservoir sizes are indicated by the side length $\mathrm{L} \cdot \mathring{\mathrm{A}}^{-1}$. For each reservoir size, the colored markers show κ_T, the solid lines are the fits of Eq. (44) to the data points, and the dotted lines are the linear equations obtained by inserting the resulting fitting parameters v^∞ and v^s from Eq. (44) into Eq. (28).

In order to examine further both contributions, we varied the total pressure of the system, between -10 and 30 MPa. The bulk contribution to the compressibility is reduced as the pressure increases (Figure 5 left panel). The same behavior is observed for the surface contribution, however, the decrease is lower, relatively speaking. The data from the Small System Method and those computed from Kirkwood-Buff integrals agree very well for the bulk contribution, and less well for the surface contributions. The result from the TIP4P/2005 model is systematically below the fit from experimental data. We attribute the deviations to the uncertainty in the computation as well as to the finite reservoir effect discussed below.

Figure 6 shows κ_T from TIP4P/2005 simulations at equal conditions for different reservoir sizes. This demonstrates how the correlation between the small system density fluctuation and the reservoir density fluctuation becomes less significant for larger reservoirs. As a consequence κ_T tends to be underestimated if the reservoir is not large enough.

For the reservoir size used to calculate κ_T in Table 4, the effect is present, but the influence is so small that it is not justified to increase the simulation time by using a larger reservoir. For the smaller reservoirs the effect extends into the regime where oscillations due to higher order terms become significant, and because of this there is no clear linear region.

Figure 7 shows the results for the application of the finite reservoir correction proposed in Eq. (44). The results are for the isothermal compressibility of TIP4P/2005 at $P = 1$ bar and $T = 298$ K. Two reservoir sizes are shown; $L = 124$ Å and $L = 62$ Å. The data points are fitted using Eq. (44) (solid lines), which gives us the finite reservoir corrected values of v^∞ and v^s. These values are subsequently inserted into Eq. (28) to show the cor-

rected slope and limit values (dotted lines). We observe that the finite reservoir effect on κ_T for the smallest reservoir is visible up to $\Omega/V \approx 0.5$, while the effect for the largest reservoir is visible up to $\Omega/V \approx 0.25$. Both reservoir sizes give the same values for v^∞ and v^s when corrected using Eq. (44).

We have thus been able to reproduce accepted values for bulk properties of water using the Small System Method. In addition, we have found results that enable us to predict how the surface contribution to the property of small volumes will vary with shape and size. Scaling laws for v, $\partial u/\partial \mu$, and κ_T have been confirmed, and the slope of the linear laws have been determined. Lastly, an equation describing the finite reservoir effect has been proposed.

7 Conclusions

A systematic investigation of the size and shape effects of some thermodynamic properties of small systems was conducted, providing a better understanding of the separate elements causing the description of these systems to deviate from classical thermodynamic systems, and improving and further developing the Small System Method. The densities and the correlations of the particle and energy densities in the small systems were accurately described as functions of size and shape with separate volume and surface terms. It was found that these quantities, which are extensive quantities in the sense of Hadwiger's theorem [10] could be written as the sum of a volume and a surface contribution.

This made it possible to obtain the value of these quantities in the thermodynamic limit. This is the property crucial for the application of the Small System Method. From these fluctuations,

thermodynamic properties such as the thermodynamic factor, partial internal energy, partial enthalpy and isothermal compressibility can be determined using standard expressions. The dependence of these properties on the volume and surface terms are then found. As these properties are not extensive quantities in the sense of Hadwiger's theorem, they can in general not be written as a simple sum of a volume and a surface contribution. The thermodynamic limit value of these quantities is found by taking the surface area zero in the available expressions. Using Hill's nanothermodynamics[1] we have shown that the volume term obtained in the limit follows classical thermodynamics, while the surface term satisfies the thermodynamics of a flat surface as described by Gibbs[4]. The shape dependence of the surface contributions of the extensive quantities in the sense of Hadwiger's theorem was verified to be proportional to the area to volume ratio of the small system. This gives the true value of the surface contribution, independent of shape.

For the small systems we consider in this paper, as well as those we considered in earlier papers[5–7,9], we find that $n^s = 0$. As we can see in Eqs. (36) and (28) this implies that the Ω/V term in the denomenators of the thermodynamic factor and the isothermal compressibility disappears. For this special case it is then possible to write the combinations in Eqs. (36) and (28) as sums of volume and surface contributions. While this is a convenient property, which we have extensively used, one should always remember that as a matter of principle the Small System Method only works properly for extensive quantities in the sense of Hadwiger's theorem.

Calculating the isothermal compressibility of water using the TIP4P/2005 model, we demonstrated, for the first time, that the method gives reasonable results also for a system with long-range interactions. The analysis of subvolumes in a closed reservoir is inherently affected by the size of the reservoir because the fluctuations in the subvolume are correlated with the fluctuations in the reservoir, and the significance of the effect increases with the fraction of reservoir volume occupied by the subvolume. A general formula for finite reservoir correction was suggested.

References

1 T. L. Hill, *The Journal of Chemical Physics*, 1962, **36**, 3182–3197.

2 T. L. Hill, *Thermodynamics of small systems, Part I*, Dover, New York, 1994.

3 T. L. Hill, *Nano Letters*, 2001, **1**, 273–275.

4 J. W. Gibbs, *The Scientific Papers of J. Willard Gibbs, Volume 1, Thermodynamics*, Ox Bow Press, Woodbridge, Connecticut, 1993.

5 S. K. Schnell, X. Liu, J.-M. Simon, A. Bardow, D. Bedeaux, T. J. H. Vlugt and S. Kjelstrup, *The Journal of Physical Chemistry B*, 2011, **115**, 10911–10918.

6 S. K. Schnell, R. Skorpa, D. Bedeaux, S. Kjelstrup, T. J. H. Vlugt and J.-M. Simon, *The Journal of Chemical Physics*, 2014, **141**, year.

7 P. Krüger, S. K. Schnell, D. Bedeaux, S. Kjelstrup, T. J. H. Vlugt and J.-M. Simon, *J. Phys. Chem. Letters*, 2013, **4**, 235–238.

8 P. Ganguly and N. F. A. van der Vegt, *Journal of Chemical Theory and Computation*, 2013, **9**, 1347–1355.

9 S. K. Schnell, T. J. Vlugt, J.-M. Simon, D. Bedeaux and S. Kjelstrup, *Molecular Physics*, 2012, **110**, 1069–1079.

10 H. Hadwiger, *Vorlesungen über Inhalt, Oberfläche und Isoperimetrie*, Springer, 1957.

11 R. Cortes-Huerto, K. Kremer and R. Potestio, *J Chem Phys*, 2016, **145**, 141103.

12 H. J. C. Berendsen, J. R. Grigera and T. P. Straatsma, *The Journal of Physical Chemistry*, 1987, **91**, 6269–6271.

13 D. J. Price and C. L. Brooks, *The Journal of Chemical Physics*, 2004, **121**, 10096–10103.

14 H. W. Horn, W. C. Swope, J. W. Pitera, J. D. Madura, T. J. Dick, G. L. Hura and T. Head-Gordon, *The Journal of Chemical Physics*, 2004, **120**, 9665–9678.

15 J. L. F. Abascal and C. Vega, *The Journal of Chemical Physics*, 2005, **123**, year.

16 A. Ben-Naim, *Molecular Theory of Solutions*, Oxford University Press, Oxford, U.K., 2005.

17 S. Plimpton, *Journal of Computational Physics*, 1995, **117**, 1 – 19.

18 M. Orsi, *Molecular Physics*, 2014, **112**, 1566–1576.

19 W. Shinoda, M. Shiga and M. Mikami, *Phys. Rev. B*, 2004, **69**, 134103.

20 G. J. Martyna, D. J. Tobias and M. L. Klein, *The Journal of Chemical Physics*, 1994, **101**, 4177–4189.

21 W. G. Hoover, *Phys. Rev. A*, 1985, **31**, 1695–1697.

22 M. Parrinello and A. Rahman, *Journal of Applied Physics*, 1981, **52**, 7182–7190.

23 J. E. R.W. Hockney, *Computer Simulation Using Particles*, IOP Publishing Ltd, 1988.

24 J.-P. Ryckaert, G. Ciccotti and H. J. Berendsen, *Journal of Computational Physics*, 1977, **23**, 327 – 341.

25 L. Ter Minassian, P. Pruzan and A. Soulard, *The Journal of Chemical Physics*, 1981, **75**, 3064–3072.

26 F. L. Ning, K. Glavatskiy, Z. Ji, S. Kjelstrup and T. J. H. Vlugt, *Phys. Chem. Chem. Phys.*, 2015, **17**, 2869–2883.

27 A. Saul and W. Wagner, *Journal of Physical and Chemical Reference Data*, 1989, **18**, 1537–1564.

28 H. L. Pi, J. L. Aragones, C. Vega, E. G. Noya, J. L. Abascal, M. A. Gonzalez and C. McBride, *Molecular Physics*, 2009, **107**, 365–374.